JSE Journal of Systematics and Evolution

doi: 10.1111/jse.12906

Research Article

# Hybridization and genome duplication for early evolutionary success in the Asian Palmate group of Araliaceae

Angélica Gallego-Narbón[1]*, Jun Wen[2], Jing Liu[3], and Virginia Valcárcel[1,4]

[1]Departamento de Biología, Universidad Autónoma de Madrid, Madrid 28049, Spain
[2]Department of Botany, National Museum of Natural History, Smithsonian Institution, Washington, DC 20560, USA
[3]College of Life Science, Sichuan Agricultural University, Ya'an 625014, Sichuan, China
[4]Centro de Investigación en Biodiversidad y Cambio Global (CIBC-UAM), Universidad Autónoma de Madrid, Madrid 28049, Spain
*Author for correspondence. E-mail: angelica.gallego@uam.es
Received 27 April 2022; Accepted 11 July 2022; Article first published online 27 July 2022

**Abstract** The phenomenal advances in sequencing techniques and analytical development during the last decade have provided a unique opportunity to unravel the evolutionary history of lineages under complex patterns of evolution. This is the case of the largest clade of the ginseng family (Araliaceae), the Asian Palmate group (AsPG), where the large internal polytomies and genome incongruences detected in previous studies pointed to a scenario of radiation with hybridization events between genera for the early evolution of the group. In this study, we aim to obtain well-resolved nuclear and plastid phylogenies of the AsPG using Hyb-Seq to evaluate the radiation hypothesis and assess the role of hybridization in the early evolution of the group. We performed concatenated- and coalescent-based phylogenetic analyses from the 936 targeted nuclear loci and 261 plastid loci obtained for 72 species representing 20 genera of the AsPG and the main clades of Araliaceae. The impact of hybridization and incomplete lineage sorting (ILS) was assessed with SNaQ, and genome duplications were evaluated with ChromEvol. Our nuclear and plastid phylogenies are compatible with a scenario of early radiation in the AsPG. Also, the identification of extensive signals of hybridization and ILS behind the genome incongruences supports hybridization as a major driving force during the early radiation. We hypothesize a whole-genome duplication event at the origin of the AsPG, followed by a radiation that led to extensive ILS, which, alongside the early inter-genera hybridization, is obscuring the phylogenetic signal in the early evolution of this major clade.

**Key words:** Araliaceae, hybridization, Hyb-Seq, incomplete lineage sorting, radiation, whole-genome duplication.

.

## 1 Introduction

Araliaceae is a diverse plant family (c. 50 genera and 1500 species) distributed mainly in tropical and subtropical latitudes (Wen et al., 2001). Phylogenetic studies have revealed three highly diversified main clades (Asian Palmate group [AsPG], *Aralia-Panax*, and *Polyscias-Pseudopanax*) as well as three less diversified early diverged clades (greater *Raukaua* clade, *Neocussonia-Astropanax* clade, and *Cussonia-Seemmanaralia* clade), six species-poor generic lineages (*Astrotricha* DC., *Cephalaralia* Harms., *Harmsiopanax* Warb., *Hydrocotyle* L., *Motherwellia* Muell., and *Osmoxylon* Miq.; Wen et al., 2001; Plunkett et al., 2004a, 2004b, 2020; Nicolas & Plunkett, 2009; Mitchell et al., 2012; Li & Wen, 2016; Gostel et al., 2017; Kadereit & Bittrich, 2018; Perkins, 2019), and two genera of unknown phylogenetic placement (*Anakasia* Philipson and *Woodburnia* Prain). The evolutionary history of the family has not yet been clarified because traditional Sanger sequencing generally failed to provide enough resolution for the internal nodes. As a result, a number of the lineages indicated above are placed in a large basal polytomy (Wen et al., 2001; Plunkett et al., 2004a, 2004b; Nicolas & Plunkett, 2009; Mitchell et al., 2012; Li & Wen, 2016). Also, the family is in constant taxonomic change including description or resurrection of several genera (e.g., *Metapanax* J. Wen & Frodin, Wen & Frodin, 2001; *Astropanax* Seem. and *Neocussonia* Hutch., Lowry et al., 2017; *Didymopanax* Decne. & Planch., Fiaschi et al., 2020), recircumscription (e.g., *Schefflera* J.R.Forst. & G.Forst., Lowry et al., 2020), or disintegration of others (e.g., *Pentapanax* Seem., Li & Wen, 2016).

The AsPG is the largest major clade of Araliaceae, including more than 50% of the genera and species of the family (23 genera, c. 930 species; Lowry et al., 2019, 2020; Valcárcel & Wen, 2019; Fiaschi et al., 2020). The AsPG is widely distributed

in Asia, Oceania, northern Africa, Europe, and the Americas across tropical and temperate latitudes. Most of the generic diversity is found in Asia, where 14 endemic genera occur alongside three other genera that expand their distribution to other continents (*Hedera* L. expands to Europe and northern Africa; *Oplopanax* (Torr. & A.Gray) Miq. to North America and *Dendropanax* Decne. & Planch. to Central and South America). Additionally, six other genera occur in Central and South America, with the Neotropics being the second richest region of the clade.

Previous studies of the AsPG using Sanger sequencing have helped resolve the species relationships within several genera, for example, *Dendropanax* (Li & Wen, 2013), *Hedera* (Ackerfield & Wen, 2003; Valcárcel et al., 2003, 2017; Valcárcel, 2008), and "*Schefflera*" (Plunkett et al., 2005, 2020; Li & Wen, 2014), while they surprisingly failed to solve the phylogenetic relationships between the genera (Wen et al., 2001; Mitchell & Wen, 2004; Plunkett et al., 2004a, 2004b, 2005, 2020; Mitchell et al., 2012; Li & Wen, 2013, 2014, 2016; Nicolas & Plunkett, 2014; Valcárcel et al., 2014). The fact that none of the Sanger studies provided enough internal resolution to clarify the backbone of the AsPG was interpreted as evidence for an ancient radiation (Valcárcel et al., 2014). Also, a pattern of topological incongruences between nuclear and plastid phylogenies was identified during this early radiation, which was interpreted as evidence for ancient hybridization events between generic lineages (Valcárcel et al., 2014; see Plunkett et al., 2020). The use of NGS techniques to analyze the complete plastid genomes (plastomes; Li et al., 2013; Valcárcel & Wen, 2019) has helped resolve the early evolutionary history of the group with persistence of low internal resolution, which strongly supports the early radiation scenario (Valcárcel & Wen, 2019). Whether this radiation was coupled with interlineage hybridization remains an open question since none of the genome-level studies conducted so far has included nuclear loci. Interestingly, one of the topological incongruences (the one affecting the phylogenetic placement of *Chengiopanax* C.B. Shang & J.Y. Huang and *Gamblea* C.B. Clarke) detected in Valcárcel et al. (2014), where only a few regions were analyzed (one nuclear and seven plastid), was later discarded when the whole plastid genome was analyzed. Indeed, the new topology obtained when the whole plastome was analyzed (Valcárcel & Wen, 2019) converged with the nuclear phylogeny obtained in Valcárcel et al. (2014).

In this study, we aim to obtain nuclear and plastid phylogenetic reconstructions of the AsPG using the NGS technique Hyb-Seq (Weitemier et al., 2014). This technique has been proven to be very effective to capture numerous loci from both plastid and nuclear genomes (Zimmer & Wen, 2015; Watson et al., 2020; Wang et al., 2021). We ultimately seek to test the radiation with interlineage hybridization hypothesis previously proposed for the AsPG (Valcárcel et al., 2014) and clarify whether hybridization played a major role in the early evolution of the group. Based on the previous plastome results, we expect to obtain the phylogenetic signal of the deep radiation in both genome reconstructions. Also, as we increase the number of nuclear loci, we expect to obtain a robust phylogenetic signal in conflict with the one obtained from the plastid genome, therefore supporting the ancient hybridization scenario. To evaluate these hypotheses, herein, we analyze 87% of the AsPG genera (including the latest taxonomic segregates of the previously broadly defined "*Schefflera*") together with representatives of all the remaining main clades of Araliaceae (greater *Raukaua* clade, *Aralia-Panax* clade and *Polyscias-Pseudopanax* clade) and a good representation of the other species-poor basally diverged clades of the family.

## 2 Material and Methods

### 2.1 Taxon sampling and library construction

A total of 72 species representing the three highly diversified clades of Araliaceae (AsPG: 53 species; *Aralia-Panax* clade: seven; *Polyscias-Pseudopanax* clade: three), two of the three poorly diversified clades (*Raukaua* clade: two species, *Astropanax*: one), and four of the eight basal generic lineages (*Cephalaralia*: one species, *Osmoxylon*: two, *Harmsiopanax*: two, *Hydrocotyle*: one) were included in this study plus *Mackinlaya schlechteri* (Harms) Philipson of Apiaceae as the outgroup (Appendix I). Therefore, our sampling covered 29 Araliaceae genera (65% of Araliaceae genera) of nine major lineages (64% of Araliaceae lineages), and 10 of the 16 remaining nonsampled Araliaceae genera were included in the sampled lineages (*Neocussonia* in Afro-Malagasy *Schefflera*; Gostel et al., 2017; *Cephalopanax*, *Frodinia*, and *Crepinella* in Neotropical *Schefflera*, Lowry et al., 2019, Plunkett et al., 2021; *Meryta*, *Neopanax*, *Plerandra*, and *Pseudopanax* in *Polyscias-Pseudopanax* clade; Li & Wen, 2016; *Cheirodendron* and *Schefflera* in *Raukaua* group, Mitchell & Wagstaff, 2000; Plunkett et al., 2005, 2020, Li & Wen, 2016). The raw reads of seven species were obtained from previous studies (six species, Valcárcel & Wen, 2019; one species from the National Agricultural Biotechnology Information Center repository from Korea; NABIC, http://nabic.rda.go.kr), whereas the remaining 65 species were newly sequenced in this study (Appendix I). The modified SDS method (Dellaporta et al., 1983) was used for DNA extraction of 62 of the 65 newly sequenced species from silica-dried material that were included in a HybSeq library. The remaining three newly sequenced species were sequenced by M. El Baidouri at the CNRS (France) using Illumina HiSeq (Illumina Inc., San Diego, USA).

A set of exon targets was designed for Araliaceae based on the comparison of the whole genomes of *Panax ginseng* (Kim et al., 2018; http://ginsengdb.snu.ac.kr/) and *Panax notoginseng* (Zhang et al., 2017; http://www.plantkingdomgdb.com/panax_notoginseng/), and the transcriptomes of *Hedera helix* and *Polyscias fruticosa* from the 1000 Plant Transcriptomes Initiative (OneKP; www.onekp.com; code: SUVN and EDBB, respectively). The selection was conducted mainly in Geneious Prime (Biomatters Ltd., Auckland, New Zealand), with a maximum *E*-value of $1 \times 10^{-10}$ for all BLAST searches. The coding regions of *P. ginseng* (ver. 1.1) and *P. notoginseng* (ver. 1) were first BLASTed against each other to identify putative orthologous genes. Only the genes present in both genomes were considered, and we accepted the genes that were strictly single copy in *P. notoginseng* and had no more than two matches in *P. ginseng*, since *P. notoginseng* is a diploid

($2n = 2x = 24$) and *P. ginseng* is a tetraploid ($2n = 4x = 48$). The selected genes were double-checked by BLASTing against their genome data and then filtered to keep those longer than 300bp and having 85%–99% of the pairwise identities between *P. ginseng* and *P. notoginseng*. The retained genes were further BLASTed against the transcriptome assemblies of *H. helix* and *P. fruticosa*, and those with multiple matches in either *H. helix* or *P. fruticosa* were excluded. Finally, 936 genes were selected, with a range from 300 to 3990 bp and a total length of 700 778 bp. For bait synthesis, we used the sequences of *P. ginseng* as the references if the genes were single copy in *P. ginseng*. Otherwise, we used the sequences of *P. notoginseng* or *H. helix*. Mybaits 120-mer biotinylated RNA probes with 3× tiling on each locus were designed and synthesized by Arbor Biosciences (Ann Arbor, MI, USA, Catalog #180912-94A). Before the synthesis, the probes were filtered by removing high repeat elements, which were identified using the PGSB (Plant Genome and Systems Biology) repeat database (Nussbaumer et al., 2012).

We pooled 6–10 indexed libraries in one reaction with equimolar amounts of 100 ng. Solution-based hybridization and enrichment were carried out following the standard MYBaits v4.01 protocol (https://arborbiosci.com/mybaits-manual/). The final enriched libraries were quantified by gel electrophoresis and a Qubit Fluorometer (Invitrogen, Carlsbad, CA, USA) using the dsDNA HS Assay Kit. To recover the plastid genome sequences, 40% of off-target libraries were added to the target-enriched libraries, and then pooled into one superpool in equimolar ratios. Sequencing with 150 bp paired-end reads was performed on an Illumina HiSeq. 4000 platform in Novogene (Davis, CA, USA).

### 2.2 Sequence capture and alignment

The obtained reads were trimmed using Trimmomatic 0.39 (Bolger et al., 2014). TriSeq 3 adapters were removed with a simple clip threshold of 10 bp, a palindrome clip threshold of 30 bp, and a seed mismatch threshold of 2bp. A quality cut-off of 15 in a 4 bp sliding window was established. All the reads under 36 bp were discarded, and bases at the beginning and the end of each read with a Phred quality score below 3 were removed. The resulting files were assembled following the HybPiper pipeline v 1.2 (Johnson et al., 2016).

To obtain nuclear data, the genes included in the designed bait set were used as the targeted genes to extract exons. Nontargeted flanking regions are considered as introns by HybPiper and were extracted using the "intronerate" function. HybPiper statistics were obtained, and potential paralogs were detected using the "paralog investigator" tool included in HybPiper. The quality of the data extracted for nuclear loci was low for the genome-skimming sequences obtained from Valcárcel & Wen (2019); therefore, only 65 species were considered for nuclear phylogenomic analyses.

To obtain plastid data, the annotated plastome of *Eleutherococcus senticosus* (Rupr. & Maxim.) Maxim. from GenBank (JN637765) was used as a reference to extract the targeted plastid genes. We used Geneious Pro 5.1.7 to add annotations to the intergenic spacers. As a result, 284 regions obtained from the annotated genome file (87 coding regions [CDS], 23 introns, 45 tRNAs + rRNAs, and 129 intergenic spacers) were used to construct the plastid targeted gene file. HybPiper was run with the default settings using this file as a reference.

The alignment was performed for each gene separately using MAFFT v7.480 (Katoh & Standley, 2013). Geneious v.9.1.3 (Kearse et al., 2012) was used to concatenate the independent alignments, obtaining 11 matrices. Six matrices were obtained for nuclear data: exons without paralogs (*NrExPn*), exons with paralogs (*NrExPy*), introns without paralogs (*NrInPn*), introns with paralogs (*NrInPy*), exons + introns without paralogs (*NrExInPn*), and exons + introns with paralogs (*NrExInPy*). Five matrices were obtained for the plastid data: plastome (*CpTot*), CDS (*CpEx*), introns (*CpIn*), tRNAs + rRNAs (*CpRna*), and intergenic spacers (*CpSpa*). Matrices were visually examined in Geneious prior to phylogenomic analyses. Statistics of each locus alignment and for the concatenated matrices were obtained using the "summary" function in AMAS 1.0 (Borowiec, 2016).

### 2.3 Phylogenomic analyses

We applied both concatenation- and coalescent-based approaches. For concatenation-based analyses, maximum likelihood (ML) was used for the 11 matrices, while Bayesian inference (BI) analyses were run only for the five plastid matrices due to computational limitations associated with the size of the nuclear alignments. ML analyses were performed in RAxML-HPC v. 8.2.10 (Stamatakis, 2014) using a GTRGAMMA model with 1000 fast bootstrap replicates. BI analyses were performed in MrBayes 3.2.6 (Huelsenbeck & Ronquist, 2001) with two runs of four Markov Chain Monte Carlo (MCMC) iterations for 50 million generations and using a GTR + G evolutionary model. Coalescent-based analyses were only run for the nuclear data. We ran RAxML for each locus separately and used ASTRAL 5.6.2. (Zhang et al., 2018) to obtain coalescent-based trees for the six nuclear matrices. Support was retrieved as local posterior probabilities ($PP_{local}$, probability of a branch to represent the species tree given a set of gene trees). Quartet scores were also retrieved for the *NrExInPn* analysis to assess tree discordance. For each quartet (an unrooted tree including four taxa), there are only three alternative topologies. The quartet scores represent the proportion of gene trees that support each of the three possible topologies that connect the four descendant lineages of any given node in a tree. The highest score of each node (Q1) indicates the proportion of loci that retrieve the most frequent topology for the four descendant lineages. The remaining quartets (Q2 and Q3) represent the proportion of loci supporting each of the two alternative topologies.

### 2.4 Branch length and paralogy

Branch lengths were quantitatively studied to assess if they were congruent with a radiation pattern (short internal branches alongside long external branches). Branch lengths based on RAxML for the nuclear (*NrExInPn*) and plastid (*CpTot*) ML phylogenies were standardized manually from 0 to 100 for easier visualization. To do this, the maximum total branch length in the AsPG from the crown of the clade was used to set the 100 value. The lengths of the AsPG internal branches were calculated as the summatory of branch lengths from the AsPG crown to the crown of the main

clades of the AsPG (hereafter *IntBracrown-clade*). The lengths of the external branches were calculated as the summatory of branch lengths from the crown of each main clade to each tip of the clade. Then, we calculated the mean of external branches per clade (hereafter *ExtBra*). To compare internal and external branch lengths per clade, we calculated the ratios between *ExtBra* and *IntBracrown-clade*. Ratios >1 indicate that branch lengths are higher between external nodes than between internal nodes, which is interpreted as a signal of radiation. To estimate the total branch length per clade from the crown of the AsPG (hereafter *AsPGcrown-Total*), we summed *ExtBra* and *IntBracrown-clade*. Then, we calculated the percentage of *ExtBra* as related to *AsPGcrown-Total* to estimate the proportion of the total branch length of the AsPG clade that lies in external branches.

For all Araliaceae samples, we calculated the total number of loci with paralogs per species and per genus, the mean number of loci with paralogs per genus, and the ratio between number of paralogs per species and the number of retrieved loci per species. We summarized these parameters in the form of violin plots and boxplots generated with the ggplot2 package (Wickham, 2016) separately for AsPG genera and non-AsPG Araliaceae genera.

### 2.5 Phylogenetic network analyses

To decouple the signals of incomplete lineage sorting (ILS) and hybridization in the nuclear data, we used SNaQ (Solís-Lemus & Ané, 2016) as implemented in PhyloNetworks (Solís-Lemus et al., 2017), which uses a pseudolikelihood approach. Due to computational limitations, we constructed a reduced nuclear dataset obtained from the 315 exon alignments of loci without paralogs (*NrExPn*), selecting 15 species representing the main AsPG clades and the basal genera of Araliaceae, using *Harmsiopanax aculeatus* (Blume) Warb. ex Boerl. as the outgroup. We constructed gene trees of the reduced matrix with RAxML and used them as the input for SNaQ analyses. We investigated the maximum number of hybridization events ($h_{max}$) with values ranging from 0 to 9, and 50 independent runs were performed per $h_{max}$ value. To assess the optimal number of hybridization events, the best network was selected for each $h_{max}$ level and the log-pseudolikelihood scores of the selected networks were plotted. According to developers (Solís-Lemus & Ané, 2016), the log-pseudolikelihood value is expected to decrease sharply as the number of hybridization events increases, until reaching the best $h_{max}$ value, and improves slowly afterward. Therefore, the phylogenetic network in which the log-pseudolikelihood score stabilizes was selected as the optimal number of hybridization events.

### 2.6 Chromosome number evolution

We used ChromEvol (Glick & Mayrose, 2014) to analyze chromosome evolution across the Araliaceae tree. We used a reduced version of our nuclear (*NrExInPn*) and plastid (*CpTot*) phylogenies including one tip per genus (29 species for the nuclear phylogeny and 30 species for the plastid phylogeny) as the input trees. Chromosome counts for the studied genera were obtained from the Index to Plant Chromosome Numbers database (IPCN; Goldblatt & Johnson, 2006) and the Chromosome Counts Database (CCDB; Rice et al., 2015) and completed with the chromosome counts on Araliaceae species reported by Yi et al. (2004). The frequency of chromosome numbers per genus was estimated from the percentage of the counts reported for each chromosome number (Data S6). We ran all the ChromEvol predefined models and selected the best one according to the AICc.

## 3 Results

### 3.1 Sequence capture success

The Hyb-Seq library allowed the recovery of a high number of reads per sample (median = 4 145 841 read pairs/sample; 62 samples), of which 80.4% persisted after trimming. We retrieved information for a mean of 876 targeted coding sequences and a total of 933 nuclear coding regions (99.7% of targeted sequences). We considered that coding regions present in less than 10 samples (i.e., 10 species) would not provide information on generic relationships and, therefore, these regions were excluded from phylogenetic analyses, which included 928 regions when paralogs were considered (*NrExPy*, *NrInPy*, and *NrExInPy* matrices). We retrieved information for 261 plastid loci (91.9% of targeted loci). Additional HybPiper statistics can be found in Data S1.

The proportion of targeted sequence recovered for each locus (Data S2) was generally high (e.g., mean of 81.6% for nuclear exons and 96.0% for chloroplast CDS). A total of 615 nuclear regions were paralogs for at least one species (Data S3). After paralog removal, we obtained 318 single-copy nuclear regions, of which 315 were present in more than 10 species and were included in *NrExPn*, *NrInPn*, and *NrExInPn* matrices. Matrix length varied from 5 198 862 bp (*NrExInPy*) to 11 232 bp (*CpRna*, Data S4). The proportion of parsimony informative sites varied from 18.5% to 24.9% in nuclear matrices (*NrExPn, NrExPy*, *NrInPn, NrInPy*, *NrExInPn, NrExInPy*) and from 0.4% to 8.8% in plastid matrices (*CpTot, CpEx, CpIn, CpRna, CpSpa*).

### 3.2 Phylogenomic analyses

Regarding the nuclear analyses including all loci and excluding paralogs (*NrExInPn*), the concatenation-based phylogeny showed an almost fully resolved AsPG tree (Fig. 1A) with all nodes highly supported (bootstrap values, BS: 99%–100%), except for three unsupported nodes, one of them internal. The same topology with higher BS for the three unsupported nodes was obtained when paralogs were included (Fig. S1A). The coalescent-based phylogeny (Fig. 2) showed a compatible AsPG tree with lower resolution as four internal nodes are unsupported or show low support ($PP_{local} = 0.81$). *Oplopanax* and the *Heptapleurum-Tetrapanax* clade were consistently recovered as consecutive sisters to a clade including the rest of the AsPG (Figs. 1A, 2). The concatenation-based phylogeny showed a deep polytomy of three main clades (the *Hedera-Merrilliopanax* clade, the *Kalopanax-Macropanax s.l.*, and a large clade including the rest of the AsPG genera, Fig. 1A). Furthermore, *Sciodaphyllum s.s.* was resolved as sister to the *Dendropanax-Gamblea* clade and the *Brassaiopsis-Trevesia* clade was sister to the *Fatsia-Oreopanax* clade (Fig. 1A). The coalescent-based ASTRAL phylogeny, however, showed the deep polytomy of five clades of AsPG: the *Hedera-Merrilliopanax* clade, the

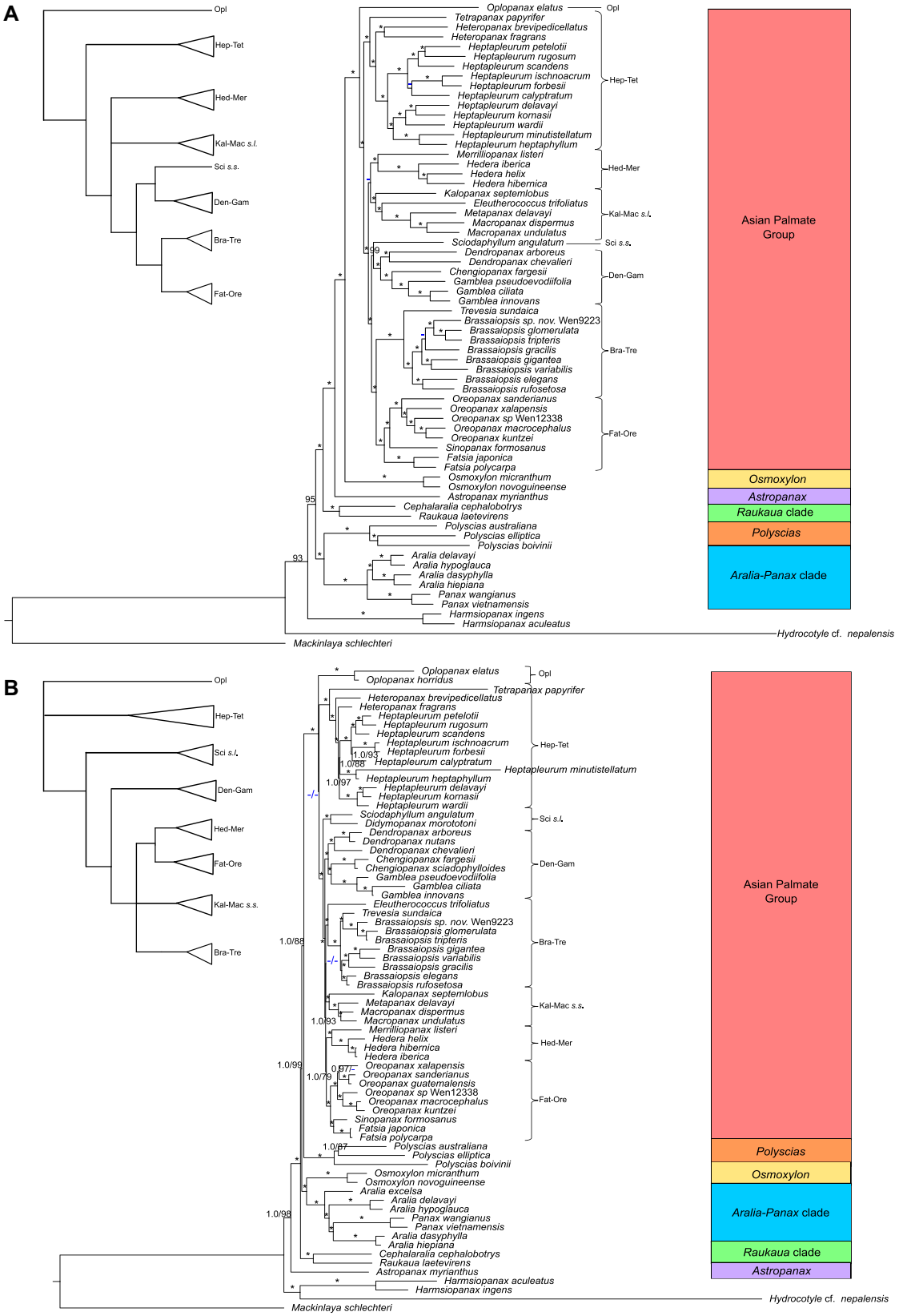


**Fig. 1.** Continued

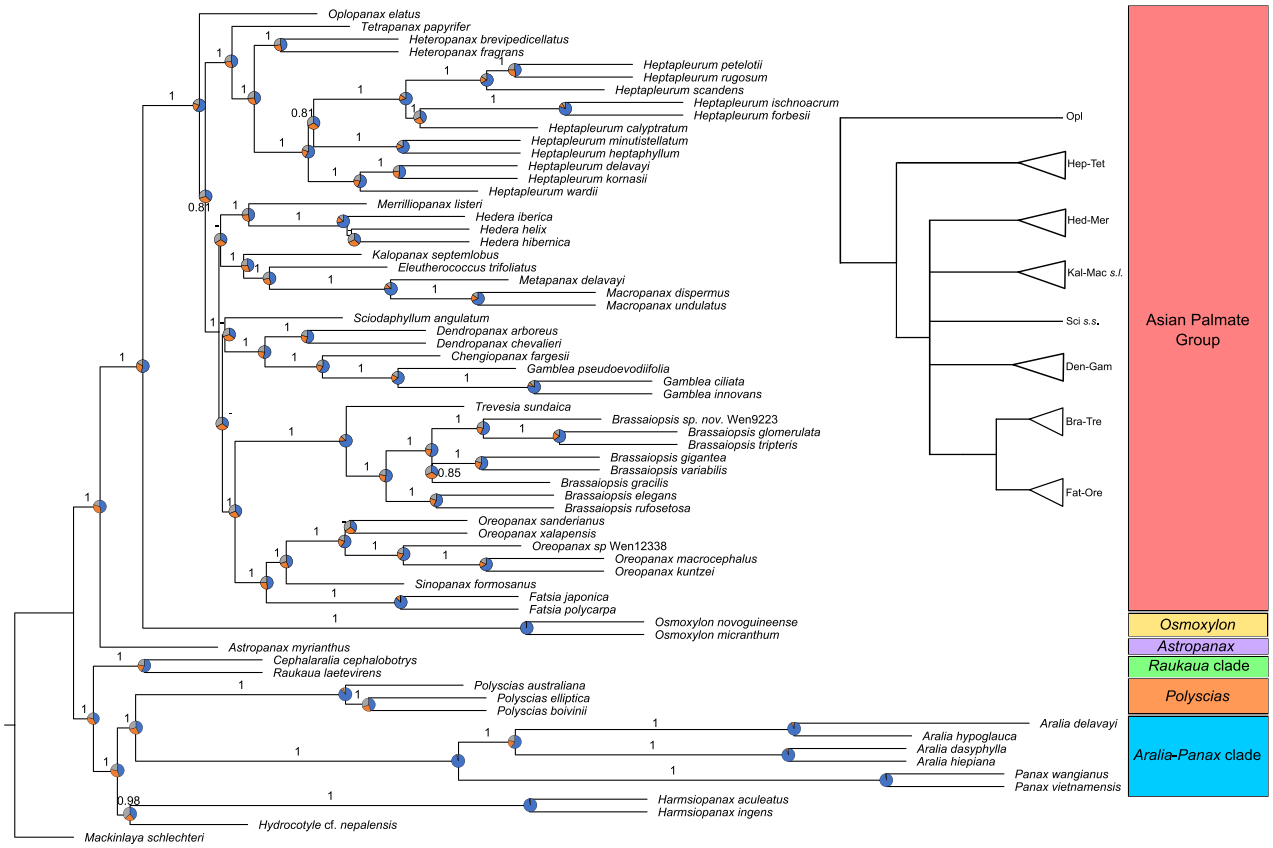


**Fig. 2.** Phylogenetic reconstructions based on the ASTRAL analysis of the complete nuclear data set including all exon (315) and intron (315) loci excluding paralogs (*NrExInPn*). Branch support is provided for all the supported branches ($PP_{local} \geq 0.8$). Hyphens indicate nonsupported branches. Quartet (i.e., unrooted tree that connects four descendants of a given node) scores are also provided: Q1 (blue) indicates the most frequent quartet recovered for a given node across all genes, and Q2 (orange) and Q3 (gray) represent the proportion of the two alternative quartets for that given node. Similar proportions of Q2 and Q3 suggest a signal of incomplete linage sorting (ILS), while different proportions of the two alternative quartets suggest a signal of hybridization. The main Araliaceae clades and the basal genera are provided. Bra-Tre, *Brassaiopsis-Trevesia* clade; Den-Gam, *Dendropanax-Gamblea* clade; Fat-Ore, *Fatsia-Oreopanax* clade; Hed-Mer, *Hedera-Merrilliopanax* clade; Hep-Tet, *Heptapleurum-Tetrapanax* clade; Kal-Mac, *Kalopanax-Macropanax* clade; Opl, *Oplopanax*; and Sci, *Sciodaphyllum.*

*Kalopanax-Macropanax* clade *s.l.* (i.e., a clade including *Kalopanax, Macropanax, Metapanax*, and *Eleutherococcus*), *Sciodaphyllum s.s.*, the *Dendropanax-Gamblea* clade, and the *Brassaiopsis-Trevesia* clade plus its sister, the *Fatsia-Oreopanax* clade (Fig. 2). The phylogenies obtained with the nuclear partitions were generally congruent with the phylogenies recovered with the complete data set both for the concatenated- and coalescent-based approaches, although some incongruences were detected mostly affecting the lineages involved in the deep polytomy of the AsPG (Figs. S1, S2). Outside the AsPG, *Osmoxylon* consistently appeared as the sister group of the AsPG in the nuclear reconstructions, and *Astropanax* was sister to the *Osmoxylon*-AsPG clade (Figs. 1A, 2). According to the concatenated-based approach, these three main Araliaceae lineages (AsPG, *Osmoxylon*, *Astropanax*) were sister to the *Raukaua* clade, and the clade formed by all of them was sister to the *Polyscias* and *Aralia-Panax* clade, with *Harmsiopanax* and *Hydrocotyle* as the consecutive sisters to all remaining Araliaceae (Fig. 1A). However, in the coalescent-based ASTRAL phylogeny, the AsPG-*Osmoxylon-Astropanax* clade was well supported, and the *Raukaua* clade was sister to a

**Fig. 1.** Phylogenetic reconstructions based on the maximum likelihood (ML) analyses of the complete nuclear (A; *NrExInPn*, i.e., with 315 exons and 315 introns without paralogs) and plastid (B; *CpTot*, i.e., 261 loci) matrices. Branch support is provided as an asterisk when bootstrap (BS) values are equal to 100 in the nuclear reconstruction or when both ML and Bayesian inference (BI) analyses show the highest support (BS = 100, PP = 1.0) for the plastid reconstruction. Hyphens indicate nonsupported branches. The main Araliaceae clades and the basal genera are provided. Bra-Tre, *Brassaiopsis-Trevesia* clade; Den-Gam, *Dendropanax-Gamblea* clade; Fat-Ore, *Fatsia-Oreopanax* clade; Hed-Mer, *Hedera-Merrilliopanax* clade; Hep-Tet, *Heptapleurum-Tetrapanax* clade; Kal-Mac, *Kalopanax-Macropanax* clade; Opl, *Oplopanax*; and Sci: *Sciodaphyllum.*

clade including (1) *Polyscias* and the *Aralia-Panax* clade and (2) a clade of *Harmsiopanax* and *Hydrocotyle* (Fig. 2).

Regarding the plastid analyses including all the retrieved loci (*CpTot*), ML and BI reconstructions provided a mostly resolved phylogeny with high support (BS: 79%–100%; posterior probabilities, PP: 0.97–1.0), except for two unsupported internal nodes (Fig. 1B). Although some incongruences were detected, the phylogenies of plastid partitions (*CpEx*, *CpIn*, *CpRna*, *CpSpa*; Fig. S3) were generally congruent with the reconstruction including all the plastid loci (Fig. 1B). *Oplopanax* was part of a basal polytomy with the *Heptapleurum-Tetrapanax* clade and a clade including the rest of the AsPG. Within this clade, *Sciodaphyllum s.l.* (i.e., the clade including *Sciadaphyllum* and *Didymopanax*; note that we could not include *Didymopanax* in the nuclear phylogeny) and the *Dendropanax-Gamblea* clades were consecutive sisters of a clade including the rest of the AsPG genera. Within the latter, a basal polytomy was recovered including three clades: the *Hedera-Merrilliopanax* clade as sister to the *Fatsia-Oreopanax* clade, the *Kalopanax-Macropanax* clade *s.s.* (i.e., excluding *Eleutherococcus*), and a clade including *Eleutherococcus* as sister to the *Brassaiopsis-Trevesia* clade. Outside of the AsPG, *Polyscias* appeared as the sister group of the AsPG, forming a clade sister to *Osmoxylon* and the *Aralia-Panax* clade (Fig. 1B). The *Raukaua* clade was sister to this main clade of Araliaceae (*AsPG-Polyscias*, *Osmoxylon-Aralia-Panax* clades), both together forming a clade sister to *Astropanax*. *Hydrocotyle* and *Harmsiopanax* formed the first diverged clade of Araliaceae.

### 3.3 Branch length and paralog distribution

The ratios between internal and external branch lengths using the main clades of crown of the AsPG (*ExtBra/IntBracrown-clade*) showed values >1 for both the nuclear (*NrExInPn*, Fig. S4C) and the plastid (*CpTot*, Fig. S4D) reconstructions, which indicates that short internal branches are followed by long external branches across the whole AsPG tree. Also, the external branches (*ExtBra*) represented 55%–89% of the total branch length from the AsPG crown (*AsPGcrownTotal*) for the nuclear phylogeny. These percentages ranged from 66% to 80% of *AsPGcrownTotal* for the plastid phylogeny. These patterns were also detected when standardized branch lengths were examined (Figs. S4A, S4B) and were congruent with a basal radiation scenario. The mean number of loci with paralogs per genus ranged from 27 to 318 for the AsPG genera (*Oplopanax* and *Merrilliopanax*, respectively) and from 50 (*Panax*) to 245 (*Raukaua*) for the non-AsPG genera (Data S5). The number of genes with paralogs was generally higher for AsPG genera both at the species level and at the genus level according to the violin plots (Fig. S5).

### 3.4 Nuclear gene conflicts: ILS and hybridization

The quartet scores retrieved by the *NrExInPn* ASTRAL analysis (Fig. 2) indicated an extended phylogenetic incongruence between gene trees from the most internal nodes of the Araliaceae tree throughout the AsPG tree, with Q1 values ranging from 34% to 98% and the lowest values located at the most internal nodes of the AsPG. Under an ILS scenario, the Q2 and Q3 values are similar, while a biased distribution of these values can be interpreted as a signal of hybridization (Schumer et al., 2016). In our phylogeny, we observed equal Q2 and Q3 values within the AsPG, suggesting extended ILS in this group, while an uneven proportion of Q2 and Q3 scores was observed for the most internal nodes of Araliaceae, which is indicative of hybridization (Fig. 2).

According to SNaQ analyses, when the networks with the lowest pseudo-likelihood for each $h_{max}$ value were compared, the optimal number of hybridization events went from three to five events, as the stabilization of the pseudo-likelihood values seems to be achieved with three hybridization events, but the lowest pseudo-likelihood was obtained with five hybridization events (Fig. S6A). However, as SNaQ was not able to perform all the runs for each level due to computational limitations, we also examined the decrease in pseudo-likelihood values for all the phylogenetic networks generated with $h_{max}$ values from 3 to 5 (Figs. S6B–S6D) and visually examined the networks near the stabilization for each $h_{max}$ level (Fig. S7). Although the vectors of inheritance probabilities varied ($\gamma$), the phylogenetic networks estimated for each $h_{max}$ value were generally similar (Figs. S7A–S7C) and all the networks detected hybridization events involving the internal nodes of the AsPG and the basal genera of Araliaceae (Figs. S7A–S7C).

### 3.5 Chromosome evolution

A total of 113 chromosome counts representative of the studied genera were compiled, ranging from 9 to 96 as the reported chromosome numbers (Data S6), and were used to construct the chromosome counts file. The best ChromEvol model was the "DysDup" model both for nuclear (AIC = 23.5209, log-likelihood = −8.7605) and plastid (AIC = 24.6142, log-likelihood = −9.30709) data (Data S7). This model assumes that three types of events are possible: whole-genome duplications (WGDs), ascending dysploidy, and descending dysploidy. The ancestral basic chromosome number estimated was 12 or 24 in all the nodes (9 nodes with $n = 12$ and 19 nodes with $n = 24$ for nuclear phylogeny, 10 nodes with $n = 12$, and 19 nodes with $n = 24$ for plastid phylogeny). The posterior probabilities for the most probable chromosome number of each node ranged from 0.59 to 1 in the nuclear reconstruction (Fig. 3A) and from 0.98 to 1 in the plastid reconstruction (Fig. 3B). Chromosome gain, chromosome loss, demi-duplication, and base-number change events were not expected for any of the nodes according to the DysDup models. The estimated rate of WGD events for the nuclear reconstruction (Fig. 3A) was <0.1 for all the nodes, except for N6 (0.32), N7 (0.28), and N8 (0.40), and 2.26 WGD events were expected according to the best model. The estimated rate of WGD events for the plastid reconstruction (Fig. 3B) was <0.1, except for N9 (0.98), and 2.32 WGD events were expected according to the best model.

## 4 Discussion

### 4.1 Hyb-Seq NGS helps resolve the backbone of the AsPG

Most of the phylogenetic studies performed in the AsPG used Sanger sequencing (i.e., Wen et al., 2001; Plunkett et al., 2004a, 2004b, 2020; Nicolas & Plunkett, 2009; Mitchell et al., 2012; Li & Wen, 2016) yielded basal polytomies at the origin of the AsPG while obtaining a good resolution for the

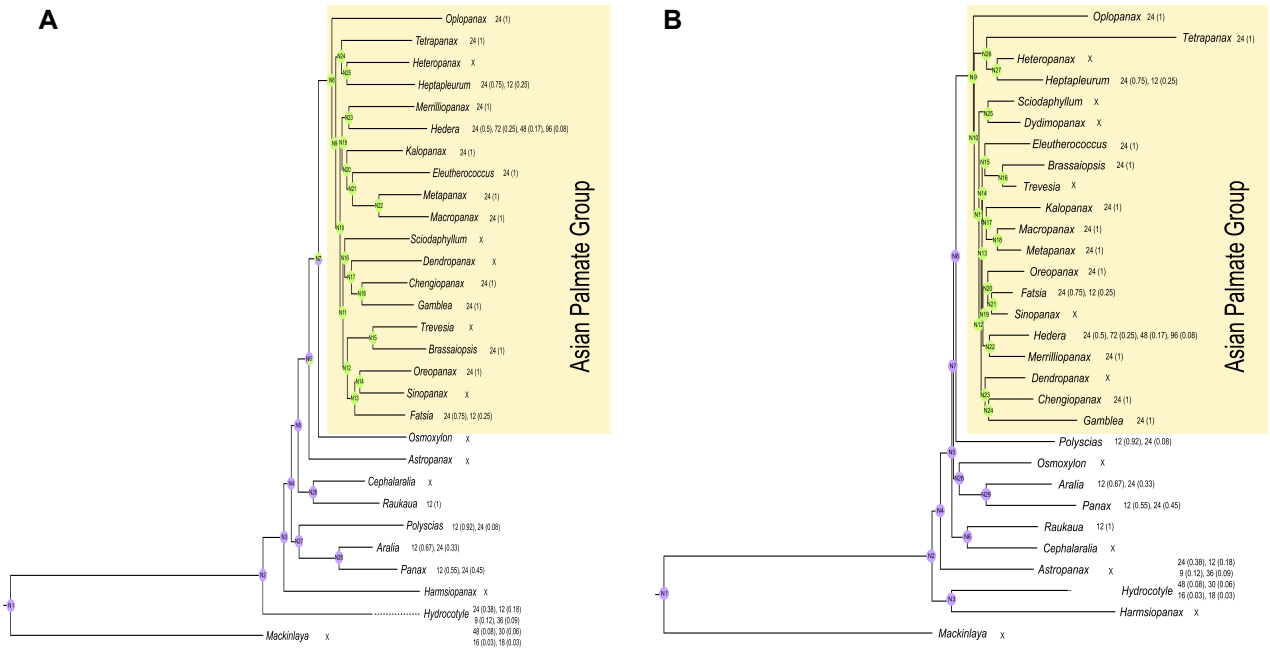


**Fig. 3.** Ancestral basic chromosome numbers inferred from nuclear (A, *NrExInPn*, Fig. 1A) and plastid (B, *CpTot*, Fig. 1B) phylogenies according to the best ChromEvol model. Purple represents the state $n = 12$ and green represents the state $n = 24$. The probability of the inferred ancestral chromosome numbers is represented by pie charts. Chromosome counts for each genus are provided if available, and "X" indicates the absence of counts for a genus. The proportion of each chromosome number per genus is provided in brackets. ChromEvol node numeration is maintained. The *Hydrocotyle* branch is not represented completely to facilitate visualization.

most external nodes. This phylogenetic pattern of resolution allowed the identification of the monophyly of most of the genera (but see Plunkett et al., 2005; Li & Wen, 2013), but it also hampered the clarification of the early evolutionary history of the group. Interestingly, the use of NGS to obtain plastome data (Li et al., 2013; Valcárcel & Wen, 2019) provided a better resolution at the base of the tree, but most of the internal nodes remained unresolved. This lack of basal resolution when using the maximum number of plastid information possible indicated that the low resolution of previous Sanger-based approaches was not a consequence of incomplete DNA sampling, but the evolutionary tracing of a rapid diversification at the origin of the group. Our NGS plastid phylogeny provided resolution for some of the nonsupported basal nodes in Valcárcel & Wen (2019), whereas the first divergence in the AsPG appears not to be well resolved (Fig. 1B). Indeed, whether the *Oplopanax* clade is sister to the big clade of *Heptapleurum-Tetrapanax* clade plus the main clade of the AsPG still needs to be tested, as it has only been weakly suggested in previous plastid phylogenies (Valcárcel et al., 2014; Li & Wen, 2016; Valcárcel & Wen, 2019; Plunkett et al., 2020).

Our previous knowledge on the nuclear phylogenetic reconstructions in the AsPG was mainly based on the use of one or two DNA regions (ITS and ETS: Plunkett et al., 2004a; ITS: Wen et al., 2001; Valcárcel et al., 2014; Plunkett et al., 2004b, 2020). These nuclear phylogenies showed a similar pattern to the one obtained in the Sanger plastid studies. In fact, the lack of basal resolution was even more extensive in the nuclear phylogenies towards more external nodes. The phylogenetic reconstructions obtained herein with 315 nuclear loci allowed the clarification of the first divergence of the AsPG, resulting in the *Oplopanax* clade as sister to the big clade consisting of the *Heptapleurum-Tetrapanax* clade plus the main clade of the AsPG (Fig. 1A) as it was previously supported in Valcárcel & Wen (2019) based on plastome data. Also, our nuclear NGS phylogeny clarifies the phylogenetic relationships among genera and allows recovery of the main clades of the AsPG, while the nuclear resolution both in Valcárcel et al. (2014) and in Plunkett et al. (2020) was mostly restricted to the most external branches. Some of the main clades of the AsPG recovered herein (the *Brassaiopsis-Trevesia* clade, the *Hedera-Merrilliopanax* clade, and the *Heptapleurum-Tetrapanax* clade) were already obtained using ITS. However, the sister-group relationship of *Dendropanax* and *Fatsia* has been retrieved in this study for the first time, as also the strong support for the phylogenetic relationship between *Kalopanax* and *Macropanax s.l.* clades. Therefore, although this NGS nuclear approach did not resolve all the internal nodes of the AsPG since the phylogenetic placement of the *Hedera-Merrilliopanax* and *Kalopanax-Metapanax s.l.* clades remains unclear, it clarified the main generic clades in the AsPG for the first time.

### 4.2 Extensive hybridization in the evolution of the AsPG lineage

Hybridization is one of the most important mechanisms of speciation in angiosperms (Soltis & Soltis, 2009). Indeed, it is widely distributed across the tree of life of flowering plants,

with certain lineages showing pervasive hybridization throughout their evolutionary history that often occurs along with polyploidization (i.e., *Lachemilla*, Morales-Briones et al., 2018; *Achillea*, Guo et al., 2005). Despite the abundant evidence of the importance of hybridization as a major microevolutionary force in different genera of Araliaceae (e.g., *Hedera*, Valcárcel et al., 2003; *Panax*, Lee & Wen, 2004), its role as a diversification force at a macroevolutionary scale in Araliaceae was overlooked until recently (Valcárcel et al., 2014). This is mostly due to technical and methodological limitations that masked the signal of hybridization in the phylogenetic reconstructions of Araliaceae. On the one hand, poor internal resolution has been systematically obtained using Sanger sequencing (Wen et al., 2001; Plunkett et al., 2005; Nicolas & Plunkett, 2009; Mitchell et al., 2012; Valcárcel et al., 2014; Li & Wen, 2016). On the other hand, the frequent use of a concatenated-based approach for the analysis of plastid and nuclear DNA sequences (but see, Plunkett et al., 2004a, 2004b) has hidden the existence of conflict signals between genomes in Araliaceae (Wen et al., 2001; Mitchell et al., 2012; Li & Wen, 2016). However, it is very likely that crossing between lineages might have played a central macroevolutionary role at least for the largest clade of Araliaceae (the AsPG) as it gathers the highest proportion of polyploids in the family (Yi et al., 2004), and its nuclear and plastid reconstructions show this conflicting signal that has been tentatively attributed to hybridization (Valcárcel et al., 2014).

Our current NGS approach recovers good internal resolution for the AsPG and hard incongruences persisted deep in the nuclear and plastid trees (Fig. 1). This conflict signal is mostly concentrated in most internal nodes of the AsPG and involves most of the generic lineages (Fig. 1). Indeed, the two genomes draw completely different histories for the early evolution of the AsPG (Fig. 1). After the divergence of *Oplopanax* and the *Heptapleurum-Tetrapanax* clade, the American *Sciodaphyllum* clade *s.l.* appears as sister to the rest of the AsPG genera according to the plastid reconstruction (Fig. 1B), while the nuclear phylogeny reveals a large basal polytomy with three main Asian clades involved (the *Hedera-Merrilliopanax* clade, the *Kalopanax-Macropanax* clade, and a clade including the rest of the AsPG clades; Fig. 1A), and the divergence of *Sciodaphyllum s.s.* occurred in a more internal position. Moreover, the *Kalopanax-Macropanax* clade and the *Hedera-Merrilliopanax* clade that occupy a relatively basal placement after the main divergence from *Sciodaphyllum* in the nuclear phylogeny (Fig. 1A) occupy more external positions in the plastid phylogeny (Fig. 1B). In summary, conflict between genomes affects most of the internal nodes of the AsPG and the divergence of most generic clades (Fig. 1). Technical issues due to limited DNA sampling are discarded as the source of conflict since our results are robustly supported from numerous loci (Nuclear data set: 315 loci, >400 000 informative positions; Plastid data set: 261 loci, >10 000; Data S4). Similarly, taxa sampling incompleteness does not seem to be the cause of incongruence as our taxonomic coverage at the genus level is almost complete (82.6% of AsPG genera in the nuclear phylogeny and 87.0% in the plastid phylogeny) and the missing genera are known to be in a lineage that is already represented in our study (*Sciodaphyllum* clade; Frodin et al., 2010; Fiaschi & Plunkett, 2011). Although paralogy (Wendel & Doyle, 1998) is extensive in the AsPG (Fig. S5, Data S3) and a frequent cause of conflict, here, it is discarded because the incongruences are detected even when paralogs are excluded (compare Figs. 1A, 1B). However, we observe a strong signal of ILS (Degnan & Rosenberg, 2009) in the nuclear loci since the quartet scores of the ASTRAL species tree for the AsPG show equal probability of the two alternative quartets for all the internal nodes of the clade (compare Q2 and Q3 in Fig. 2). Given that the phylogenetic reconstruction obtained from the nuclear loci is affected by ILS, part of the incongruence detected between the nuclear and plastid phylogenies can be attributed to ILS, which is likely given the short time for speciation that affected the divergence of most generic lineages during the early radiation proposed for the origin of the AsPG (see below; Valcárcel et al., 2014, Valcárcel & Wen, 2019). However, it is not the sole cause since nuclear reconstructions under the coalescent- and concatenated-based approaches are compatible (compare Figs. 1A, 2) and both are incongruent with the plastid tree (Fig. 1B). Indeed, when the effect of hybridization is decoupled from ILS, the best networks detected are those with multiple hybridization events (between 3 and 5), with some of the detected hybridization events affecting the conflicting internal nodes of the AsPG (Figs. S6, S7). Altogether, we interpret the genome incongruences in the AsPG as the phylogenetic signal of multiple events of ancient hybridization between generic lineages that occur in a short period of time with fast proliferation of lineages, during which there was not enough time to complete lineage sorting. In fact, most of the phylogenetic networks retrieved two hybridization events at the origin of the AsPG. Hybridization between genera seems plausible, as intergeneric hybrids have been artificially obtained in the AsPG (i.e., × *Fatshedera*; Knobloch, 1972). Therefore, it is likely that genetic and genomic barriers were also naturally defeated in the past, provided that physical contact between lineages was possible. Although the biogeographical hypothesis needs to be revisited in the light of our nuclear results, previous ancestral reconstructions placed the first ancestors after the divergence of the *Oplopanax* clade and the *Heptapleurum-Tetrapanax* clade at the same intercontinental broad area (Valcárcel & Wen, 2019), which would make the physical contact possible despite the large intercontinental disjunctions of current distributions and help explain the lack of resolution between the clades formed by *Oplopanax* clade, *the Heptapleurum-Tetrapanax* clade, and the clade including the rest of the AsPG in our plastid phylogeny. A good example of an early hybridization process is inferred from the different placement of the neotropical genus *Sciodaphyllum*, with a sister relationship with the largest clade of the AsPG (the one including all AsPG genera except *Oplopanax*, *Heptapleurum*, and *Heteropanax*) in the plastid phylogeny (Fig. 1B), or as sister to the *Dendropanax-Gamblea* clade in the nuclear phylogeny (Fig. 1A). The nuclear topology is more congruent with geography, with both *Dendropanax* and *Sciodaphyllum* containing neotropical taxa. However, the plastid topology is more congruent with morphology as *Sciodaphyllum* is morphologically highly distinctive from *Dendropanax*, while it is similar to the genus *Heptapleurum* that diverged early

within the AsPG clade. Indeed, previous classifications placed taxa of *Sciodaphyllum* and *Heptapleurum* in the large genus *Schefflera* until very recently (Lowry & Plunkett, 2020). In addition, most of the obtained SNaQ networks (Fig. S7) suggest that *Sciodaphyllum* was the result of a hybridization involving the base of the AsPG, which would explain the different placements of this genus in the nuclear and plastid phylogenies. A good example of more recent evidence of hybridization between lineages is inferred from the different placements of *Sinopanax* within the *Oreopanax-Fatsia* clade. Our plastid results indicate that *Sinopanax* is sister to *Fatsia* (Fig. 1B), while according to the nuclear topology, it is sister to *Oreopanax* (Fig. 1A), which is consistent with previous results on the AsPG (Wen et al., 2001, Plunkett et al., 2004a, 2004b). This case is challenging since *Sinopanax* and *Fatsia* are Asian endemics, while *Oreopanax* occurs in the Neotropics. Interestingly, the two Asian genera are poorly diversified (one species of *Sinopanax* and three species of *Fatsia*), while the neotropical *Oreopanax* is highly diversified (c. 150 species). Hybrid speciation has been linked to niche shifts allowing colonization and diversification in new environments (Nolte & Tautz, 2010), which could be the case of *Oreopanax*.

Hybridization is not only recovered for the early diversification of the AsPG. Instead, there is evidence of hybridization across the whole tree of Araliaceae. Indeed, phylogenetic conflicts are observed from shallow positions in the tree (e.g., incongruences within *Hedera, Heptapleurum*, or *Polyscias*, or within the *Fatsia-Oreopanax* clade) to the deep nodes of the family (Figs. 1A, 1B). Previous molecular phylogenies were inconclusive regarding the early evolution in Araliaceae because the main clades of the family (AsPG, the *Aralia-Panax* clade, *Osmoxylon*, and *Polyscias*) appeared in a large deep polytomy together with a series of species-poor clades (Wen et al., 2001; Plunkett et al., 2005; Mitchell et al., 2012; Nicolas & Plunkett, 2014). In this study, we have included 65% of Araliaceae genera (i.e., 29 of the 45 Araliaceae genera). Although this percentage may seem too low to reach conclusions at the family level, the genera selected covered all the highly diversified main clades of Araliaceae and 55% of the poorly diversified and single generic clades (Wen et al., 2001; Plunkett et al., 2005; Mitchell et al., 2012; Nicolas & Plunkett, 2014). Besides, 10 of the 16 nonsampled genera have a robust phylogenetic placement within one of the clades sampled herein, as previous phylogenetic studies indicate (Fiaschi & Plunkett, 2011; Li & Wen, 2016; Plunkett et al., 2020). Therefore, with 65% of the Araliaceae genera sampled herein, we represent 64% of the main lineages of Araliaceae. Interestingly, while we provide a fully resolved tree among all the main clades and the poorly diversified lineages of Araliaceae (Fig. 1), the early evolution in Araliaceae remains unclear because of the conflicts detected between genomes at the deep nodes (Figs. 1, 2). Indeed, all the Araliaceae clades included in our study apart from the AsPG (*Aralia-Panax*, *Polyscias-Pseudopanax*, *Raukaua*, *Osmoxylon*, and *Astropanax*) show phylogenetic incongruences between nuclear and plastid phylogenies (Figs. 1, 2). Interestingly, one of these incongruences affects the origin of the AsPG. Indeed, while the sister of the AsPG in the nuclear phylogeny is the clade of *Osmoxlyon*, according to the plastid phylogeny, its sister is the clade of *Polyscias* (Figs. 1A, 1B). This suggests that hybridization was also likely for the origin of the whole AsPG clade, and probably accounted for the origin of the remaining main lineages of Araliaceae. The footprint of hybridization is observed in the biased distribution of quartet scores Q2 and Q3 deep in the Araliaceae ASTRAL phylogeny (Fig. 2). When there is a significant difference in the proportions of Q2 and Q3 for a node, as it is the case for the most internal nodes of Araliaceae (Fig. 2), this can be interpreted as a signal of hybridization, leading to a biased gene flow and one of the minor topologies being more supported than expected (Schumer et al., 2016). Additional evidence of hybridization behind the incongruence detected is the multiple hybridization events detected with SNaQ (Figs. S6, S7). However, this result should be interpreted with caution because of the reported limitations of the software in detecting hybridizations as the number of events increases (Solís-Lemus & Ané, 2016). Indeed, the hybridization events detected with SNaQ are not fully congruent with the hybridization events suggested by the conflicts detected between genomes (Figs. 1A vs. 1B). Nevertheless, our results provide evidence of extensive hybridization across the AsPG group and for the remaining Araliaceae clades.

### 4.3 Was ancient polyploidy a driver for rapid evolutionary success in the AsPG?

During the last 15 years, we have observed phenomenal advances in phylogenetic statistical methods paralleled with the revolution of NGS techniques that bypass Sanger technical issues to recover robust phylogenies and detect radiations (see Soltis & Soltis, 2019 for revision). Thus, our knowledge on the impact of radiations in evolution and diversity has grown exponentially in the last decade (Simões et al., 2016). Indeed, we are aware that Darwin's "abominable mystery" about the rapid diversification of angiosperms is the result of a pattern of nested radiations scattered across time and lineages, but starting as early as in the origin of core eudicots (Soltis & Soltis, 2004; Landis et al., 2018). From the multiple examples of radiated lineages currently documented, we know that radiations can be triggered by many different factors (Simões et al., 2016; Soltis & Soltis, 2019), such as biotic interactions in the form of co-evolutionary processes like the one between insect pollinators and the diversification of angiosperms (Dilcher, 2000) or the combination of biotic and abiotic interactions resulting in amazing oceanic island radiations like the paradigmatic case of the Hawaiian silverwoods (Baldwin, 1997). Yet, the reason why some lineages experienced recurrent radiations and some others do not remains a mystery.

Our results point to a nested pattern of radiations in Araliaceae as has already been proposed for the order Apiales (Tank et al., 2015). Although we obtained almost fully resolved reconstructions, a constant pattern of short internal branches, followed by long external branches (Fig. S4) is observed not only in the AsPG but also in the deepest nodes of the Araliaceae tree (Figs. 1, S1–S3). This pattern, which is compatible with the phylogenetic signal of an ancient radiation (Whitfield & Lockhart, 2007), is particularly stressed in the AsPG and provides additional evidence from the nuclear genome to support the early radiation of the AsPG already identified based on plastome data (Valcárcel &

Wen, 2019). Interestingly, some of the short internal branches involved in this early radiation are also associated with the conflicting signals due to hybridization and ILS patterns that were detected for the nuclear gene conflicts (see above, Figs. 1, 2). Thus, we now have strong evidence to link the early rapid diversification of the AsPG with major events of interlineage hybridization that led to the main genera of the group as already suggested (Valcárcel et al., 2014). Furthermore, we also observe a pattern of short internal branches and long external branches at the origin of Araliaceae leading to the main clades and the species-poor clades of the family (Figs. 1, S4). Our sampling of Araliaceae outside the AsPG is limited; hence, our conclusions on the early diversification of the family are preliminary and need to be tested further (but see above). However, this result may point to an ancient radiation in Araliaceae as well, which is congruent with the increase in the diversification rate that was detected for the family (Tank et al., 2015). This hypothesis is not new since previous phylogenetic studies already suggested that Araliaceae experienced an early radiation (Plunkett et al., 2004a, 2004b; Yi et al., 2004). Given that several lineages involved in this early radiation of Araliaceae also show incongruent placements (Figs. 1A vs. 1B) and hybridization events (Fig. S7), we suggest that hybridization between generic lineages was also important for the early diversification of the family, not just within the AsPG. Interestingly, the ancient hybridization between the clades of *Osmoxylon* and *Polyscias* involved in the origin of the AsPG (Figs. 1A vs. 1B) concurred with a WGD event (Fig. 3). This result is not surprising, given that WDGs are one of the most frequent mechanisms of postzygotic stabilization after hybridization (Stebbins, 1947) and the highest proportion of polyploids in Araliaceae occurs in the AsPG. Indeed, Yi et al. (2004) advocated for an ancient polyploidization for the AsPG based on the distribution of polyploids and diploids in the Araliaceae tree.

Our results suggest that Araliaceae underwent two nested radiations in which hybridization acted as a major evolutionary force. This finding fits well in the general pattern observed in angiosperms, where multiple lineages show recurrent radiations (i.e., Cracraft & Donoghue, 2004; Davies et al., 2004; Moore et al., 2010). Although the reason why these radiations tend to occur bounded within a lineage is still unknown (Soltis et al., 2019), the fact that most of these lineages are preceded by ancient WGDs (Tank et al., 2015; Landis et al., 2018) points to genomic bases as a likely explanation. Neither Tank et al. (2015) nor Landis et al. (2018) detected an increase in the diversification rate in Araliaceae, but they both recovered high net diversification rates and low net extinction rates for this family that was, indeed, identified as a species-rich descendant lineage. Interestingly, Landis et al. (2018) detected one WGD in the lineage of Apiales at the divergence between Pittosporaceae, Araliaceae, and Apiaceae. Therefore, it is plausible to assume that, as in other angiosperm lineages with radiations, WGD may have contributed to the generation of novelties that drove the radiations observed herein. Indeed, this WGD in Apiales (Landis et al., 2018) can also be linked to the nested radiations proposed herein for Araliaceae, assuming the WGD time-lag hypothesis (Schranz et al., 2012). This hypothesis suggests that the novelties that arose after a WGD event may persist silenced in the descendant lineages and only after a certain period of time do the subsequent evolutionary events provide the opportunity for the evolutionary success of the particular descendant lineage involved, resulting in a radiation. The WGD-lag time hypothesis has been suggested for numerous lineages of angiosperms (Tank et al., 2015; Soltis & Soltis, 2019) and whether it is the case for Araliaceae needs to be further investigated.

## Acknowledgements

The authors are grateful to M. El Baidouri for sequencing the *Hedera* samples, Gabriel Johnson for assistance with library construction and target enrichment experiments, C. Benítez-Benítez for her help with data assembly, and Zelong Nie for his assistance with SNaQ analyses. We also thank P. P. Lowry for providing updated taxonomic information of the genera that were included in "*Schefflera*." This study was financed in part by the Spanish Ministry of Economy, Industry, and Competitiveness (CGL2017-87198-P), the Spanish Ministry of Science and Innovation (PID2019-106840GA-C22), the Laboratories of Analytical Biology of the Smithsonian Institution, and the Smithsonian Institution DNA Barcode Network. A. Gallego-Narbón was supported by the program "Contratos predoctorales para Formación de Personal Investigador FPI-UAM" of Universidad Autónoma de Madrid (FPI-UAM 2018) and the Smithsonian Institution Fellowship Program (SIFP).

## Data Availability Statement

The raw reads (FASTQ files) used in this study are available in the NCBI Sequence Read Archive (SRA) database (Bioproject ID: PRJNA841627).

## References

Ackerfield J, Wen J. 2003. Evolution of *Hedera* (the ivy genus, Araliaceae): Insights from chloroplast DNA data. *International Journal of Plant Sciences* 164: 593–602.

Baldwin BG. 1997. Adaptive radiation of the Hawaiian silversword alliance: Congruence and conflict of phylogenetic evidence from molecular and nonmolecular investigations. In: Givnish TJ, Sytstma KJ eds. *Molecular evolution and adaptive radiation*. Cambridge, UK: Cambridge University Press. 103–128.

Bolger AM, Lohse M, Usadel B. 2014. Trimmomatic: A flexible trimmer for Illumina sequence data. *Bioinformatics* 30: 2114–2120.

Borowiec ML. 2016. AMAS: A fast tool for alignment manipulation and computing of summary statistics. *PeerJ* 4: e1660.

Cracraft J, Donoghue MJ. 2004. *Assembling the tree of life*. New York: Oxford University Press.

Davies TJ, Barraclough TG, Chase MW, Soltis PS, Soltis DE, Savolainen V. 2004. Darwin's abominable mystery: Insights from a supertree of the angiosperms. *Proceedings of the National Academy of Sciences USA* 101: 1904–1909.

Degnan JH, Rosenberg NA. 2009. Gene tree discordance, phylogenetic inference and the multispecies coalescent. *Trends in Ecology & Evolution* 24: 332–340.

Dellaporta SL, Wood J, Hicks JB. 1983. A plant DNA minipreparation: Version II. *Plant Molecular Biology Reporter* 1: 19–21.

Dilcher D. 2000. Toward a new synthesis: Major evolutionary trends in the angiosperm fossil record. *Proceedings of the National Academy of Sciences USA* 97: 7030–7036.

Eom SH, Lee JK, Kim H, Hyun TK. 2017. De novo transcriptomic analysis to reveal functional genes involved in triterpenoid saponin biosynthesis in Oplopanax elatus NAKAI. *Journal of Applied Botany and Food Quality* 90: 18–24.

Fiaschi P, Lowry PP, Plunkett GM. 2020. Studies in Neotropical Araliaceae. III. Resurrection of the New World genus *Didymopanax* Decne. & Planch., previously included in *Schefflera* (Araliaceae). *Brittonia* 72: 16–22.

Fiaschi P, Plunkett GM. 2011. Monophyly and phylogenetic relationships of neotropical *Schefflera* (Araliaceae) based on plastid and nuclear markers. *Systematic Botany* 36: 806–817.

Frodin DG, Lowry II PP, Plunkett GM. 2010. *Schefflera* (Araliaceae): Taxonomic history, overview and progress. *Plant Diversity and Evolution* 128: 561–595.

Glick L, Mayrose I. 2014. ChromEvol: Assessing the pattern of chromosome number evolution and the inference of polyploidy along a phylogeny. *Molecular Biology and Evolution* 31: 1914–1922.

Goldblatt P, Johnson DE eds. 2006. Index to plant chromosome numbers 2001-2003. In: *Monographs in systematic botany from the Missouri Botanical Garden*. St. Louis, Mo: Missouri Botanical Garden Press. 106: 1–242.

Gostel MR, Plunkett GM, Lowry PP. 2017. Straddling the Mozambique channel: Molecular evidence for two major clades of Afro-Malagasy *Schefflera* (Araliaceae) co-occurring in Africa and Madagascar. *Plant Ecology and Evolution* 150: 87–108.

Guo Y, Saukel J, Mittermayr R, Ehrendorfer F. 2005. AFLP analyses demonstrate genetic divergence, hybridization, and multiple polyploidization in the evolution of *Achillea* (Asteraceae-Anthemideae). *New Phytologist* 166: 273–290.

Huelsenbeck JP, Ronquist F. 2001. MrBayes: Bayesian inference of phylogenetic trees. *Bioinformatics* 17: 754–755.

Johnson MG, Gardner EM, Liu Y, Medina R, Goffinet B, Shaw AJ, Zerega NJC, Wickett NJ. 2016. HybPiper: Extracting coding sequence and introns for phylogenetics from high-throughput sequencing reads using target enrichment. *Applications in Plant Sciences* 4: 1600016.

Kadereit JW, Bittrich V. 2018. *The families and genera of vascular plants. Volume XV. Apiales, Gentianales (except Rubiaceae)*. Cham, Switzerland: Springer.

Katoh K, Standley DM. 2013. MAFFT multiple sequence alignment software version 7: Improvements in performance and usability. *Molecular Biology and Evolution* 30: 772–780.

Kearse M, Moir R, Wilson A, Stones-Havas S, Cheung M, Sturrock S, Buxton S, Cooper A, Markowitz S, Duran C, Thierer T, Ashton B, Meintjes P, Drummond A. 2012. Geneious basic: An integrated and extendable desktop software platform for the organization and analysis of sequence data. *Bioinformatics* 28: 1647–1649.

Kim N-H, Jayakodi M, Lee S-C, Choi B-S, Jang W, Lee J, Kim HH, Waminal NE, Lakshmanan M, van Nguyen B, Lee YS, Park H-S, Koo HJ, Park JY, Perumal S, Joh HJ, Lee H, Kim J, Kim IS, Kim K, Kodoru L, Kang KB, Sung SH, Yu Y, Parl DS, Choi D, Seo E, Kim S, Kim Y-C, Hyun DY, Park Y-I, Kim C, Lee T-H, Kim HU, Soh MS, Lee Y, In JG, Kim H-S, Kim Y-M, Yang D-C, Wing RA, Lee D-Y, Paterson AH, Yang T-J. 2018. Genome and evolution of the shade-requiring medicinal herb *Panax ginseng*. *Plant Biotechnology Journal* 16: 1904–1917.

Knobloch IW. 1972. Intergeneric hybridization in flowering plants. *Taxon* 21: 97–103.

Landis JB, Soltis DE, Li Z, Marx HE, Barker MS, Tank DC, Soltis PS. 2018. Impact of whole-genome duplication events on diversification rates in angiosperms. *American Journal of Botany* 105: 348–363.

Lee C, Wen J. 2004. Phylogeny of *Panax* using chloroplast *trnC–trnD* intergenic region and the utility of trnC–trnD in interspecific studies of plants. *Molecular Phylogenetics and Evolution* 31: 894–903.

Li R, Ma P-F, Wen J, Yi T-S. 2013. Complete sequencing of five araliaceae chloroplast genomes and the phylogenetic implications. *PLoS One* 8: e78568.

Li R, Wen J. 2013. Phylogeny and Biogeography of *Dendropanax* (Araliaceae), an amphi-pacific disjunct genus between tropical/subtropical Asia and the Neotropics. *Systematic Botany* 38: 536–551.

Li R, Wen J. 2014. Phylogeny and biogeography of Asian *Schefflera* (Araliaceae) based on nuclear and plastid DNA sequence data: Phylogeny and biogeography of Asian *Schefflera*. *Journal of Systematics and Evolution* 52: 431–449.

Li R, Wen J. 2016. Phylogeny and diversification of Chinese Araliaceae based on nuclear and plastid DNA sequence data: Phylogeny and diversification of Chinese Araliaceae. *Journal of Systematics and Evolution* 54: 453–467.

Lowry PP, Plunkett GM. 2020. Resurrection of the genus *Heptapleurum* for the Asian Clade of species previously included in *Schefflera* (Araliaceae). *Novon* 28: 143–170.

Lowry PP, Plunkett GM, Gostel MR, Frodin DG. 2017. A synopsis of the Afro-Malagasy species previously included in *Schefflera* (Araliaceae): Resurrection of the genera *Astropanax* and *Neocussonia*. *Candollea* 72: 265.

Lowry PP, Plunkett GM, Mora MM, Cano A, Fiaschi P, Frodin DG, Gereau RE, Idárraga-Piedrahíta Á, Jiménez-Montoya J, Mendoza JMF, Neill DA, Rivera-Diaz O, Rodrigues-Vaz C. 2020. Studies in Neotropical Araliaceae. I. Resurrection of the genus *Sciodaphyllum* P. Browne to accommodate most New World species previously included in *Schefflera* J. R. Forst. & G. Forst. *Brittonia* 72: 1–15.

Lowry PP, Plunkett GM, Neill DA. 2019. Studies in Neotropical Araliaceae. II. Resurrection of the neotropical genus *Crepinella* for a clade of new world species previously Included in *Schefflera* (Araliaceae). *Novon* 27: 253–261.

Mitchell A, Li R, Brown JW, Schönberger I, Wen J. 2012. Ancient divergence and biogeography of *Raukaua* (Araliaceae) and close relatives in the southern hemisphere. *Australian Systematic Botany* 25: 432.

Mitchell A, Wagstaff SJ. 2000. Phylogeny and biogeography of the Chilean *Pseudopanax laetevirens*. *New Zealand Journal of Botany* 38: 409–414.

Mitchell A, Wen J. 2004. Phylogenetic utility and evidence for multiple copies of Granule-Bound Starch Synthase I (GBSSI) in Araliaceae. *Taxon* 53: 29–41.

Moore MJ, Soltis PS, Bell CD, Burleigh JG, Soltis DE. 2010. Phylogenetic analysis of 83 plastid genes further resolves the early diversification of eudicots. *Proceedings of the National Academy of Sciences USA* 107: 4623–4628.

Morales-Briones DF, Liston A, Tank DC. 2018. Phylogenomic analyses reveal a deep history of hybridization and polyploidy in the Neotropical genus *Lachemilla* (Rosaceae). *New Phytologist* 218: 1668–1684.

Nicolas AN, Plunkett GM. 2009. The demise of subfamily Hydrocotyloideae (Apiaceae) and the re-alignment of its genera across

the entire order Apiales. *Molecular Phylogenetics and Evolution* 53: 134–151.

Nicolas AN, Plunkett GM. 2014. Diversification times and biogeographic patterns in Apiales. *Botanical Review* 80: 30–58.

Nolte AW, Tautz D. 2010. Understanding the onset of hybrid speciation. *Trends in Genetics* 26: 54–58.

Nussbaumer T, Martis MM, Roessner SK, Pfeifer M, Bader KC, Sharma S, Gundlach H, Spannagl M. 2012. MIPS PlantsDB: A database framework for comparative plant genome research. *Nucleid Acids Research* 41: 1144–1151.

Perkins AJ. 2019. Molecular phylogenetics and species delimitation in annual species of *Hydrocotyle* (Araliaceae) from South Western Australia. *Molecular Phylogenetics and Evolution* 134: 129–141.

Plunkett GM, Chandler GT, Lowry II PP, Pinney SM, Sprenkle TS. 2004a. Recent advances in understanding Apiales and a revised classification. *South African Journal of Botany* 70: 371–381.

Plunkett GM, Lowry PP, Fiaschi P, Frodin DG, Nicolas AN. 2020. Phylogeny, biogeography, and morphological evolution among and within the Neotropical and Asian clades of *Schefflera* (Araliaceae). *Taxon* 68: 1278–1313.

Plunkett GM, Lowry PP, Frodin DG, Wen J. 2005. Phylogeny and geography of Schefflera: Pervasive polyphyly in the largest genus of Araliaceae. *Annals of the Missouri Botanical Garden* 92: 202–224.

Plunkett GM, Lowry PP, Neil DA. 2021. Studies in Neotropical Araliaceae. VII. Two new genera, *Cephalopanax* and *Frodinia*, to accommodate the remaining species of Neotropical *Schefflera*. *Brittonia* 73: 251–261.

Plunkett GM, Wen J, Lowry II PP. 2004b. Infrafamilial classifications and characters in Araliaceae: Insights from the phylogenetic analysis of nuclear (ITS) and plastid (trnL-trnF) sequence data. *Plant Systematics and Evolution* 245: 1–39.

Rice A, Glick L, Abadi S, Einhorn M, Kopelman NM, Salman-Minkov A, Mayzel J, Chay O, Mayrose I. 2015. The Chromosome Counts Database (CCDB)—A community resource of plant chromosome numbers. *New Phytologist* 206: 19–26.

Schranz EM, Mohammadin S, Edger PP. 2012. Ancient whole genome duplications, novelty and diversification: The WGD radiation lag-time model. *Current Opinion in Plant Biology* 15: 147–153.

Schumer M, Cui R, Powell DL, Rosenthal GG, Andolfatto P. 2016. Ancient hybridization and genomic stabilization in a swordtail fish. *Molecular Ecology* 25: 2661–2679.

Simões M, Breitkreuz L, Alvarado M, Baca S, Cooper JC, Heins L, Herzog K, Lieberman BS. 2016. The evolving theory of evolutionary radiations. *Trends in Ecology & Evolution* 31: 27–34.

Solís-Lemus C, Ané C. 2016. Inferring phylogenetic networks with maximum pseudolikelihood under incomplete lineage sorting. *PLoS Genetics* 12: e1005896.

Solís-Lemus C, Bastide P, Ané C. 2017. PhyloNetworks: A package for phylogenetic networks. *Molecular Biology and Evolution* 34: 3292–3298.

Soltis DE, Soltis PS. 2019. Nuclear genomes of two magnoliids. *Nature Plants* 5: 6–7.

Soltis PS, Folk RA, Soltis DE. 2019. Darwin review: Angiosperm phylogeny and evolutionary radiations. *Proceedings of the Royal Society B: Biological Sciences* 286: 20190099.

Soltis PS, Soltis DE. 2004. The origin and diversification of angiosperms. *American Journal of Botany* 91: 1614–1626.

Soltis PS, Soltis DE. 2009. The role of hybridization in plant speciation. *Annual Review of Plant Biology* 60: 561–588.

Stamatakis A. 2014. RAxML version 8: A tool for phylogenetic analysis and post-analysis of large phylogenies. *Bioinformatics* 30: 1312–1313.

Stebbins GL. 1947. Types of polyploids: Their classification and significance. *Advances in Genetics* 1: 403–429.

Tank DC, Eastman JM, Pennell MW, Soltis PS, Soltis DE, Hinchliff CE, Brown JW, Sessa EB, Harmon LJ. 2015. Nested radiations and the pulse of angiosperm diversification: Increased diversification rates often follow whole genome duplications. *New Phytologist* 207: 454–467.

Valcárcel V. 2008. *Taxonomy, systematics and evolution of* Hedera L. *(Araliaceae)*. Ph.D. Dissertation. Spain: Pablo de Olavide University.

Valcárcel V, Fiz O, Vargas P. 2003. Chloroplast and nuclear evidence for multiple origins of polyploids and diploids of *Hedera* (Araliaceae) in the Mediterranean basin. *Molecular Phylogenetics and Evolution* 27: 1–20.

Valcárcel V, Fiz-Palacios O, Wen J. 2014. The origin of the early differentiation of ivies (*Hedera* L.) and the radiation of the Asian Palmate group (Araliaceae). *Molecular Phylogenetics and Evolution* 70: 492–503.

Valcárcel V, Guzmán B, Medina NG, Vargas P, Wen J. 2017. Phylogenetic and paleobotanical evidence for late Miocene diversification of the tertiary subtropical lineage of ivies (*Hedera* L., Araliaceae). *BMC Evolutionary Biology* 17: 1–14.

Valcárcel V, Wen J. 2019. Chloroplast phylogenomic data support Eocene amphi-Pacific early radiation for the Asian Palmate core Araliaceae. *Journal of Systematics and Evolution* 57: 547–560.

Wang HX, Morales-Briones DF, Moore MJ, Wen J, Wang HF. 2021. A phylogenomic perspective on gene tree conflict and character evolution in Caprifoliaceae using target enrichment data, with Zabelioideae recognized as a new subfamily. *Journal of Systematics and Evolution* 59: 897–914.

Watson LE, Siniscalchi CM, Mandel J. 2020. Phylogenomics of the hyperdiverse daisy tribes: Anthemideae, Astereae, Calenduleae, Gnaphalieae, and Senecioneae. *Journal of Systematics and Evolution* 58: 841–852.

Weitemier K, Straub SCK, Cronn RC, Fishbein M, Schmickl R, McDonnell A, Liston A. 2014. Hyb-seq: Combining target enrichment and genome skimming for plant phylogenomics. *Applications in Plant Sciences* 2: 1400042.

Wen J, Frodin DG. 2001. *Metapanax*, a new genus of Araliaceae from China and Vietnam. *Brittonia* 53: 116–121.

Wen J, Plunkett GM, Mitchell AD, Wagstaff SJ. 2001. The evolution of Araliaceae: A phylogenetic analysis based on ITS sequences of nuclear ribosomal DNA. *Systematic Botany* 26: 144–167.

Wendel JF, Doyle JJ. 1998. Phylogenetic incongruence: Window into genome history and molecular evolution. In: Soltis DE, Soltis PS, Doyle JJ eds. *Molecular systematics of plants II*. Boston, MA: Springer US. 265–296.

Whitfield JB, Lockhart PJ. 2007. Deciphering ancient rapid radiations. *Trends in Ecology & Evolution* 22: 258–265.

Wickham H. 2016. *Ggplot2: Elegant graphics for data analysis*. New York: Springer-Verlag.

Yi T, Lowry PP, Plunkett GM, Wen J. 2004. Chromosomal evolution in Araliaceae and close relatives. *Taxon* 53: 987–1005.

Zhang C, Rabiee M, Sayyari E, Mirarab S. 2018. ASTRAL-III: Polynomial time species tree reconstruction from partially resolved gene trees. *BMC Bioinformatics* 19: 153.

Zhang D, Li W, Xia E, Zhang Q, Liu Y, Zhang Y, Tong Y, Zhao Y, Niu Y, Xu J, Gao L-Z. 2017. The medicinal herb *Panax notoginseng* genome provides insights into ginsenoside biosynthesis and genome evolution. *Molecular Plant* 10: 903–907.

Zimmer EA, Wen J. 2015. Using nuclear gene data for plant phylogenetics: Progress and prospects II. Next-gen approaches:

Nuclear data for plant phylogenetics II. *Journal of Systematics and Evolution* 53: 371–379.

## Supplementary Material

The following supplementary material is available online for this article at http://onlinelibrary.wiley.com/doi/10.1111/jse.12906/suppinfo:

**Fig. S1**. Concatenation-based phylogenetic trees for nuclear partitions.

**Fig. S2**. Coalescent-based phylogenetic trees for nuclear partitions.

**Fig. S3**. Phylogenetic trees for plastid partitions.

**Fig. S4.** Estimates on standardized branch lengths.

**Fig. S5.** Violinplots of paralog distribution in AsPG genera and non-AsPG genera.

**Fig. S6.** SNaQ pseudo-likelihood values for each of the $h_{max}$ levels tested.

**Fig. S7.** Best SNaQ networks with three, four, and five hybridization events.

**Data S1.** Hyb-Piper statistics.

**Data S2.** Proportion of targeted sequences recovered for each locus.

**Data S3.** Genes with paralog warnings according to HybPiper.

**Data S4.** Alignment statistics according to AMAS.

**Data S5.** Paralog summary per genus in AsPG and non-AsPG genera.

**Data S6.** Compilation of chromosome counts of the Araliaceae family.

**Data S7.** Parameters or ChromEvol models for nuclear and plastid chromosome number reconstructions.

**Appendix I.** List of materials used in the nuclear and plastid Hyb-Seq study.

| Species | Locality | Voucher |
|---|---|---|
| *Aralia dasyphylla* Miq. | Indonesia, Java, Cibodas Botanical Garden area | *Wen 10129* |
| *Aralia delavayi* J.Wen | China, Yunnan, Bingchuan | *Wen 3040* |
| *Aralia excelsa* (Griseb.) J.Wen | Costa Rica, Parque Nacional Santa Rosa | *Wen 6779** |
| *Aralia hiepiana* J.Wen & Lowry | Vietnam, Lam Dong Prov. | *Wen 11004* |
| *Aralia hypoglauca* (C.J.Qi & T.R.Cao) J.Wen & Y.F.Deng | China, Hunan | *Deng Y.F. s.n* |
| *Astropanax myrianthus* (Baker) Lowry, G.M.Plunkett, Gostel & Frodin | Madagascar, Antsiranana, National Montagne d′ Ambre | *Wen 9570* |
| *Brassaiopsis elegans* Ridl. | Malaysia, Selangor. Raub - Kuala Kubu Bharu | *Wen 8408* |
| *Brassaiopsis gigantea* J.Wen & Lowry | Vietnam, Hoa Binh Prov. | *Wen 10941* |
| *Brassaiopsis glomerulata* (Blume) Regel | Vietnam, Vinh Phuc Prov. | *Wen 10821* |
| *Brassaiopsis gracilis* Hand.-Mazz. | Vietnam, Lao Cai Prov. | *Wen 10859* |
| *Brassaiopsis rufosetosa* (Ridl.) Jebb | Malaysia, Pahang, Peng Lai Xian Jin Chinese Temple | *Wen 8406* |
| *Brassaiopsis* sp. nov. | China, Tibet, Pailong Xiang | *Wen 9223* |
| *Brassaiopsis tripteris* (H.Lév.) Rehder | China, Guangxi, Huanjiang Xian (Niujiaozhai) | *Wen 13741* |
| *Brassaiopsis variabilis* C.B.Shang | Vietnam, Ninh Binh Prov. | *Wen 10907* |
| *Cephalaralia cephalobotrys* (F.Muell.) Harms | Australia, New South Wales, World of the Blue Mountains | *Wen 12186* |
| *Chengiopanax fargesii* (Franch.) C.B.Shang & J.Y.Huang | China, Hunan, Zhiyunshan Nature Preserve | *Wen 9316* |
| *Chengiopanax sciadophylloides* (Franch. & Sav.) C.B.Shang & J.Y.Huang | Japan, Honshu | *Soejima s.n.* |
| *Dendropanax arboreus* (L.) Decne. & Planch. | Jamaica | *Wen 11843* |
| *Dendropanax chevalieri* (R.Vig.) Merr. | Vietnam, Lao Cai Prov. | *Wen 10844* |
| *Dendropanax nutans* (Sw.) Decne. & Planch. | Jamaica | *Wen 11878* |
| *Didymopanax morototoni* (Aubl.) Decne. & Planch. | Bolivia, Cochabamba. vicinity of Hotel Victoria | *Nee & Wen 53964** |
| *Eleutherococcus trifoliatus* (L.) S.Y.Hu | China, Hubei, Changyang Xian | *Wen 14527* |
| *Fatsia japonica* (Thunb.) Decne. & Planch. | China, Zhejiang, Hangzhou Botanical Garden | *Wen 11148* |
| *Fatsia polycarpa* Hayata | China, Taiwan, Taoyuan Hsiang | *Wen 9391* |
| *Gamblea ciliata* C.B.Clarke in J.D.Hooker | China, Hunan, Luohandong | *Wen 9334* |
| *Gamblea innovans* (Siebold & Zucc.) C.B.Shang, Lowry & Frodin | Japan, Honshu | *Soejima 1094* |
| *Gamblea pseudoevodiifolia* (K.M.Feng) C.B.Shang, Lowry & Frodin | Vietnam, Lao Cai Prov. | *Wen 10850* |
| *Harmsiopanax aculeatus* (Blume) Warb. ex Boerl. | Indonesia, Java, Cibodas Botanical Garden area | *Wen 10130* |
| *Harmsiopanax ingens* Philipson | Papua New Guinea, Morobe Province, Mt. Kolorong area | *Wen 12309* |
| *Hedera helix* L. | Spain, Málaga, Ronda | *04VV20‡* |
| *Hedera hibernica* (G. 5 Kirchner) Bean | Spain, Cordoba, Trasierra | *11VV20‡* |
| *Hedera iberica* (McAll.) Ackerf. & J.Wen | Spain, Huelva, Fuenteheridos | *11VV18‡* |
| *Heptapleurum calyptratum* (Hook. f. & Thomson) Y. F. Deng | Vietnam, Lam Dong Prov. | *Wen 11061* |
| *Heptapleurum delavayi* Franch. | China, Sichuan, Mt. Omei | *Wen 12106* |
| *Heptapleurum forbesii* (Ridl.) Lowry & G. M. Plunkett | China, Sichuan, Mt. Omei | *Wen 12130* |
| *Heptapleurum heptaphyllum* (L.) Y. F. Deng | China, Guangdong, Wutongshan | *Wen 12816* |
| *Heptapleurum ischnoacrum* (Harms) Lowry & G. M. Plunkett | Papua New Guinea, Eastern Highlands | *Wen 12350* |
| *Heptapleurum kornasii* (Grushv. & Skvortsova) Lowry & G. M. Plunkett | Vietnam, Lam Dong Prov. | *Wen 11045* |
| *Heptapleurum minutistellatum* (Merr. ex H. L.Li) Y. F. Deng | China, Guangdong, Nankunshan | *Wen 13291* |
| *Heptapleurum petelotii* (Merr.) G. M. Plunkett & Lowry | Vietnam, Ninh Binh Prov. | *Wen 10946* |
| *Heptapleurum rugosum* (Blume) Boerl. | Indonesia, West Java Province, Bogor Botanical Garden | *Wen 10158* |
| *Heptapleurum scandens* (Blume) Seem. | Indonesia, Java, Cibodas Botanical Garden area | *Wen 10128* |
| *Heptapleurum wardii* (C. Marquand & Airy Shaw) G. M. Plunkett & Lowry | China, Tibet, Xizang Province. Linzhi Xian, Pailong Xiang, on slopes behind Pailong Xiang | *Wen 9224* |
| *Heteropanax brevipedicellatus* H.L.Li | China, Guangdong, Nankunshan | *Wen 13266* |

| Species | Locality | Voucher |
|---|---|---|
| *Heteropanax fragrans* (Roxb.) Seem. | Vietnam, Ninh Binh Prov. | *Wen 10905* |
| *Hydrocotyle nepalensis* Hook. | China, Taiwan, Taoyuan Hsiang | *Wen 9401* |
| *Kalopanax septemlobus* (Thunb.) Koidz. | China, Hubei, Yichang Shi | *Wen 14561* |
| *Mackinlaya schlechteri* (Meisn.) Philipson | Papua New Guinea, Eastern Highlands | *Wen 12331* |
| *Macropanax dispermus* (Blume) Kuntze | Indonesia, Bali, Gunong Batukau | *Wen 12422* |
| *Macropanax undulatus* (Wall. ex G.Don) Seem. | China, Yunnan, Tiantou Chun. | *Wen 10569* |
| *Merrilliopanax listeri* (King) H.L.Li | China, Yunnan, Gaoligong Mountains | *Wen 6326-4* |
| *Metapanax delavayi* (Franch.) J.Wen & Frodin | China, Yunnan, Qianjia Cong | *Wen 9146* |
| *Oplopanax elatus* (Nakai) Nakai | Korea, Korea Forest Research Institute | s.n[†] |
| *Oplopanax horridus* (Sm.) Miq. | USA, Alaska | *Taylor s.n.** |
| *Oreopanax guatemalensis* (Lem. ex Bosse) Decne. & Planch. ex Witte | Mexico, Chiapas, Ixhuatan. Ixhuatan. | *Wen 8736** |
| *Oreopanax kuntzei* Harms ex Kuntze | Bolivia, Cochabamba, Río Ivirizu | *Wen 53910* |
| *Oreopanax macrocephalus* Decne. & Planch. ex Wedd. | Bolivia, Cochabamba, Dept. Cochabamba, Monte Punco | *Wen 53909* |
| *Oreopanax sanderianus* Hemsl. | Mexico, Oaxaca, El Porvenir | *Wen 8691* |
| *Oreopanax sp* | Mexico | *Wen 12338* |
| *Oreopanax xalapensis* (Kunth) Decne. & Planch. | Mexico, Oaxaca, along Rt. 175, San Miguel Suchixtepec | *Wen 8689* |
| *Osmoxylon micranthum* (Harms) Philipson | Papua New Guinea, Eastern Highlands | *Wen 12341* |
| *Osmoxylon novoguineense* (Scheff.) Becc. | Indonesia, Irian Barat, Keerom | *Wen 10706* |
| *Panax vietnamensis* Ha & Grushv. | Vietnam, Lam Dong Prov. | *Jing Liu 49* |
| *Panax wangianus* S.C.Sun | China, Sichuan, Mt. Omei | *Wen 12167* |
| *Polyscias australiana* (F.Muell.) Philipson | Indonesia, Irian Barat, Keerom | *Wen 10710* |
| *Polyscias boivinii* (Seem.) Bernardi | Madagascar, Antsiranana, Montagne des Francais | *Wen 9633* |
| *Polyscias elliptica* (Blume) Lowry & G.M.Plunkett | Indonesia, West Java Province, Bogor Botanical Garden | *Wen 10157* |
| *Raukaua laetevirens* (Gay) Frodin | Chile originally, cult. | *Wen 2019306* |
| *Sciadophyllum angulatum* (Pav.) Poir. | Peru, Oxapampa | *Wen 8589* |
| *Sinopanax formosanus* (Hayata) H.L.Li | China, Taiwan, Taoyuan Hsiang | *Wen 9395* |
| *Tetrapanax papyrifer* (Hook.) K.Koch | China, Zhejiang, Qingyuan Xian, Wudabao Xiang, Honguang Village | *Wen 11233* |
| *Trevesia sundaica* Miq. | Indonesia, West Java Province, Bogor Botanical Garden | *Wen 10162* |

Locality, voucher, and accession numbers are provided for each sample. Asterisks indicate samples not included in the nuclear phylogeny. All voucher specimens are deposited at the United States National Herbarium (US), except for *Hedera* species, available at the herbarium of Universidad Autónoma de Madrid (MAUAM). *Samples obtained from Valcárcel & Wen (2019); [†]Sample obtained from NABIC (NN-2578, Eom et al., 2017); [‡]Samples provided by M. El Baidouri.